

COUPLING CLASSICAL CARRIER TRANSPORT, CAPTURE, AND SIZE QUANTIZATION IN A QUANTUM WELL LASER SIMULATOR

Matt Grupen and Karl Hess

The Beckman Institute

Department of Electrical and Computer Engineering

University of Illinois

405 N. Mathews Ave., Urbana, IL 61801, 217-333-9734

Abstract

A model for the coupling of the classical and quantum regions of a quantum well laser diode is presented. The calculation of carrier transport in different regions of the laser is first discussed. Then a discretization of the carrier continuity equations in and around the quantum well is presented in detail. The model is finally tested through the simulation of three different *GaAs/AlGaAs* lasers. The results are discussed, and the importance of carrier capture is demonstrated.

I. INTRODUCTION

There are several different approaches to quantum well laser simulation. One approach is based on the Statz-de Mars rate equations [1] and is widely used because of its simplicity and flexibility. However, it can not be used to calculate the actual transport of carriers, and therefore it can not yield local variations in the carrier densities. An alternative approach involves the self-consistent solution of the semiconductor equations with carrier transport. Several such simulators have been produced for a two-dimensional cross section of the laser [2,3,4]. Some self-consistent simulators use drift-diffusion theory throughout the entire device [5], while others have complemented drift-diffusion theory with thermionic emission theory at abrupt heterojunctions [2,4]. However, the code presented in this paper is the only laser simulator that treats the capture of carriers and size quantization in the quantum well.

This paper will discuss the simulation of carrier transport in the laser simulator called Minilase. In particular, the numerical implementation of capture and quantization will be presented in detail. Modulation responses will then be calculated by Minilase to illustrate the importance of carrier capture.

II. THE LASER MODEL

The device equations for a laser diode consist of those that describe the carrier dynamics and those that describe the photon dynamics. The carrier dynamics can be expressed by Poisson's equation and the continuity equations for electrons and holes. Since the spatial distributions of free carriers in the quantum well are determined by size quantization, Schrödinger's equation for the conduction and valence subbands must also be solved in this region [6].

The photon dynamics can be calculated by including optical gain, spontaneous emission, and cavity losses in a photon rate equation for each longitudinal mode. The mode gain and spontaneous emission are determined by the amount of inversion, the optical matrix element, and the photon

density. The inversion charge is determined by the carrier dynamics, and the optical matrix element can be calculated from Fermi's Golden Rule [7]. The photon populations can be mapped into local photon densities through the solution of Maxwell's equations for the laser cavity [6].

Since the continuity equations include the divergence in carrier flux, carrier transport must be calculated throughout the device. Because the electric field is normally moderate in the bulk regions of the device, the parabolic band approximation and drift-diffusion theory are appropriate in these regions [8]. Abrupt heterojunctions, however, are modeled in Minilase as discontinuities in the band edges. Carrier fluxes at such discontinuities are better calculated with the ballistic transport found in thermionic emission theory [9]. This theory requires a carrier injected from one material into another to immediately scatter into thermal equilibrium with the carriers in the latter material. This is a good approximation for a single heterojunction because most carriers will inelastically scatter within a mean free path after crossing the interface.

Since the quantum well is the region of optical gain, it is very important to accurately calculate the carrier dynamics in and around this region. Drift-diffusion theory can be used in the surrounding bulk regions, and ballistic transport determines the injection of carriers into the well. However, since the size of the well is on the order of a mean free path, thermionic emission must be augmented to account for the probability that a carrier traverses the well without inelastic scattering. This can be done by carefully discretizing the quantum well as shown in figure 1.

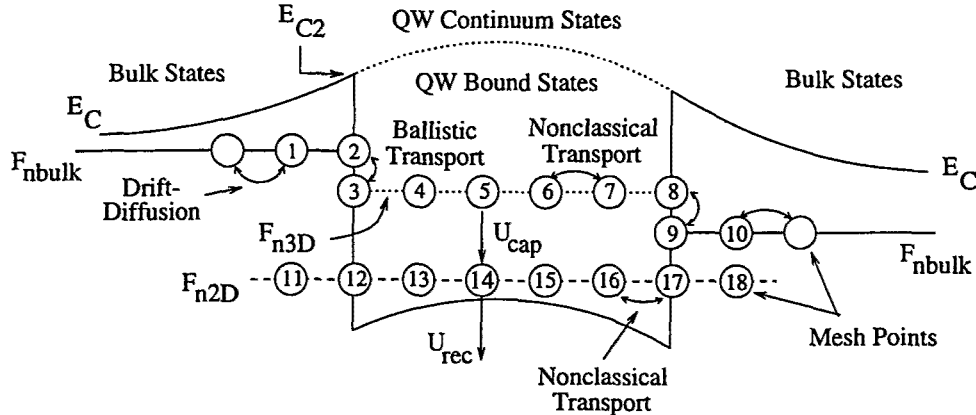


Figure 1: A schematic diagram showing the discretization of the quantum well and its coupling to the classical regions.

The quantum well must be partitioned into the continuum states above the well and the lower energy bound states. Our choice of the boundary between continuum and bound states is neither purely classical nor quantum mechanical. It accounts in part for quantum reflections, and quantum resonances are incorporated through the scattering rate between the two partitions. Associated with each partition is a unique quasi-Fermi level. Carriers injected from the bulk into the quantum well are restricted to the continuum states. This ballistic injection can be easily calculated from the quasi-Fermi levels for the bulk and the continuum using an expression similar to thermionic emission. For example, using the node numbers in the figure,

$$j_{n,2 \rightarrow 3} = A^* T^2 \left[\exp \left(\frac{F_{nbulk,2} - E_{C2}}{kT} \right) - \exp \left(\frac{F_{n3D,3} - E_{C2}}{kT} \right) \right] \quad (1)$$

A carrier in the continuum can transfer back into the classical region via an analogous expression, or it can inelastically scatter and be captured into a bound state. The scattering process is modeled with a net capture term similar to Hall-Shockley-Read recombination [10]. The spatial distributions of quantum well carriers are determined by their wave functions. The continuum wave functions are approximated by plane waves, and those in the bound states are obtained from Schrödinger's

equation. Also, according to size quantization, all the mesh points in the continuum must have the same quasi-Fermi levels, and similarly F_{n2D} must be constant.

To illustrate the discretization of the quantum well, the electron continuity equations for the continuum and the bound states, discretized in one dimension, are shown below. The two-dimensional case is analogous. First, let us pick the continuum node 5 (any continuum node can be chosen). The equation for this node is then

$$\sum_{i=3}^8 \frac{\partial n_i}{\partial t} l_i = j_{n,2 \rightarrow 3} - j_{n,8 \rightarrow 9} - \sum_{i=3}^8 U_{cap,i} l_i \quad (2)$$

where l_i is the length associated with node i according to the box integration method [11]. The equations for continuum points $j=3,4,6,7,8$ are simply $F_{n3D,j} = F_{n3D,5}$. Similarly, let us pick bound mesh point 14. Its continuity equation is

$$\sum_{i=11}^{18} \frac{\partial n_i}{\partial t} l_i = \sum_{i=11}^{18} (U_{cap,i} - U_{rec,i}) l_i \quad (3)$$

and the equations for bound points $j=11 \rightarrow 13, 15 \rightarrow 18$ are simply $F_{n2D,j} = F_{n2D,14}$.

Although the quantum well mesh points that share the same real space coordinates have different quasi-Fermi levels, the electrostatic potential is single valued and is determined by the total charge at each real space coordinate. To illustrate, let us pick heterojunction node 2 (nodes 3 or 12 could also have been picked) and write the discrete Poisson's equation in one dimension.

$$0 = \sum_{i=1,4} \epsilon_{2,i} \frac{\psi_2 - \psi_i}{|x_2 - x_i|} - (N_{D,2}^+ - N_{A,2}^-)(l_2 + l_3) - \sum_{j=2,3,12} (p_j - n_j) l_j \quad (4)$$

Note that node 2 belongs to the bulk and node 3 belongs to the continuum. Therefore, $l_2 = (x_2 - x_1)/2$ and $l_3 = (x_4 - x_3)/2$ according to the box integration method. Since the bound states overlap into the bulk regions, $l_{12} = (x_{13} - x_{11})/2$. Equation (4) determines ψ at node 2, and the potentials at nodes 3 and 12 immediately follow because ψ is continuous (to a very close approximation) at the interface, i.e. $\psi_j = \psi_2$ where $j=3,12$.

III. Results

The importance of the carrier dynamics in and around the quantum well is made very clear by the modulation response. To demonstrate this, three 100 Å *GaAs* single quantum well laser diodes were simulated. One diode contained an *Al_{0.3}Ga_{0.7}As* separate confinement region (SCR) measuring 1450 Å on each side of the well. Another diode contained an SCR that measured 2950 Å on each side. In the third device, the SCR was asymmetric, measuring 2950 Å on the *p*-side and 950 Å on the *n*-side. The results are shown in figure 2. The frequencies and heights of the resonant peaks are influenced by photon dynamics. The rates of roll-off near zero frequency, however, are directly related to carrier capture, and they differ for the three devices. Reducing the size of the *n*-side has caused the asymmetric device to roll off more gradually than the wide device. This is due primarily to the number of holes that were not captured by the well. Figure 3 shows these holes for the two devices. These carriers are not used to modulate the optical output power but, instead, contribute to parasitic diffusion capacitance. The number of wasted holes is clearly smaller for the asymmetric device, and therefore this device has smaller diffusion capacitance and a more gradual roll-off in the modulation response.

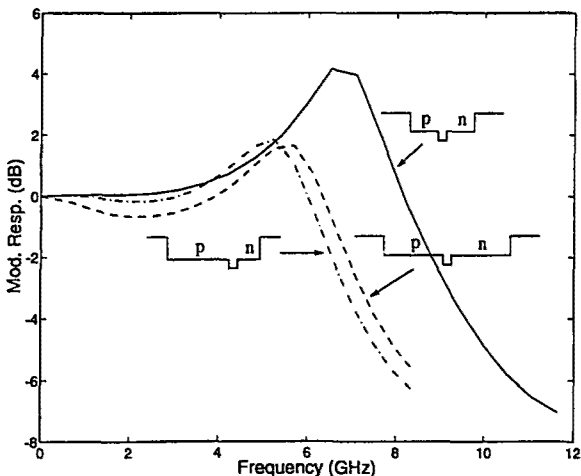


Figure 2: Modulation responses for three different separate confinement regions.

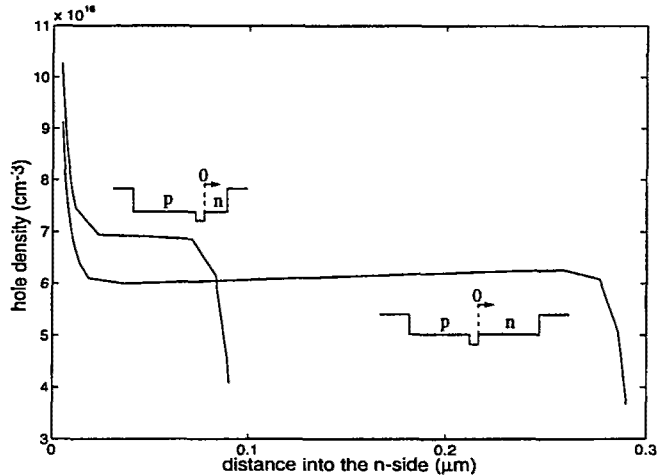


Figure 3: Hole densities on the *n*-sides of the asymmetric and wide lasers.

IV. Conclusions

An accurate simulation of a quantum well laser diode requires the treatment of carrier and photon dynamics throughout the entire device. The carrier dynamics can be calculated by treating transport appropriately in different regions of the laser. Coupling the quantum well to the surrounding bulk regions is particularly critical because it determines the pumping of the active region. We have described a model which permits the simulation of classical transport in bulk regions as well as size quantization and carrier capture in the quantum well. Furthermore, we have presented a discretization of this model that is suitable for numerical solution.

This work was funded by NSF support through the NCCE.

- [1] H. Stattz and G. de Mars, in *Quantum Electronics*, edited by C.H. Townes, (Columbia University Press, New York, 1960), p. 530.
- [2] G.H. Song, K. Hess, T. Kerkhoven, and U. Ravaioli, *Europ. Trans. Telecomm. Related Tech.*, **1**, 375 (1990).
- [3] S. Seki, T. Yamanaka, and K. Yokoyama, *J. Appl. Phys.*, **71**, 3572 (1992).
- [4] Z.M. Li, K.M. Dzurko, A. Delâge, and S.P. McAlister, *IEEE J. Quantum Electron.*, **28**, 792 (1992).
- [5] T. Ohtoshi *et al.*, *Solid-State Electron.*, **30**, 627 (1987).
- [6] M. Grupen, U. Ravaioli, A. Galick, K. Hess, and T. Kerkhoven, in *Proceedings of the SPIE OE/LASE Conference, Los Angeles* (SPIE, Bellingham, WA, 1994).
- [7] G. Lasher and F. Stern, *Phys. Rev.*, **133**, A533 (1964).
- [8] K. Hess, *Advanced Theory of Semiconductor Devices* (Prentice Hall, Englewood Cliffs, NJ, 1988).
- [9] M. Grupen, K. Hess, and G.H. Song, in *Simulation of Semiconductor Devices and Processes, Vol. 4*, edited by V. Fichtner and D. Aemmer (Hartung-Gorre Verlag, Konstanz, Germany, 1991), p. 303.
- [10] M. Grupen, G. Kosinovsky, and K. Hess, in *Proceedings of the International Electron Device Meeting, Washington, DC* (IEEE, New York, 1993) p. 23.6.1.
- [11] S. Selberherr, *Analysis and Simulation of Semiconductor Devices* (Springer-Verlag, Wien-New York, 1984).